Dielectric study of the antiplasticization of trehalose by glycerol

A. Anopchenko, T. Psurek, D. VanderHart, J. F. Douglas,* and J. Obrzut†
Polymers Division, National Institute of Standards and Technology, Gaithersburg, Maryland 20899, USA
(Received 27 January 2006; revised manuscript received 8 April 2006; published 7 September 2006)

Recent measurements have suggested that the antiplasticizing effect of glycerol on trehalose can significantly increase the preservation times of proteins stored in this type of preservative formulation. In order to better understand the physical origin of this phenomenon, we examine the nature of antiplasticization in trehalose-glycerol mixtures by dielectric spectroscopy. These measurements cover a broad frequency range between 40 Hz to 18 GHz (covering the secondary relaxation range of the fragile glass-former trehalose and the primary relaxation range of the strong glass-former glycerol) and a temperature (T) range bracketing room temperature (220 K to 350 K). The Havriliak-Negami function precisely fits our relaxation data and allows us to determine the temperature and composition dependence of the relaxation time τ describing a relative fast dielectric relaxation process appropriate to the characterization of antiplasticization. We observe that increasing the glycerol concentration at fixed T increases τ (i.e., the extent of antiplasticization) until a temperature dependent critical "plasticization concentration" x_{wp} is reached. At a fixed concentration, we find a temperature at which antiplasticization first occurs upon cooling and we designate this as the "antiplasticization temperature," T_{ant}. The ratio of the τ values for the mixture and pure trehalose is found to provide a useful measure of the extent of antiplasticization, and we explore other potential measures of antiplasticization relating to the dielectric strength.

DOI: 10.1103/PhysRevE.74.031501 PACS number(s): 64.70.Pf

I. INTRODUCTION

Sugars have been utilized to preserve foods since ancient times and more recently it has been recognized that some sugars are particularly effective preservatives of biological materials. The discovery of these "special" sugars arose from the investigation of the survival of organisms in extreme hot and cold environments. Recent studies have shown that trehalose is effective in preserving and maintaining the activity of diverse materials including proteins, viruses, and antibodies subject to drying [1] and that sugar formulations are generally effective in preserving biological tissue [2] and drugs [3].

Since preservative properties of trehalose are evidently of significant practical interest in the preservation of foods, organs and tissue, and drugs, there has correspondingly been a surge in studies dedicated to understanding and optimizing these properties. Glass formation is certainly an effective way to slow down large-scale molecular transport and thus an enhancement of preservation times can naturally be expected in formulations with a high glass transition temperature T_g [4]. The high T_g of trehalose has been recognized as a factor enhancing the preservation time [5,6]. Recent measurements and simulations have shown that even the internal motions of proteins and other biological macromolecules tend to be strongly coupled to those of the solutions in which they are embedded [7–9]. It is natural to expect that solutions having a high T_g would also be effective in protein preservation, and some authors have suggested that this is a primary factor in the increased stability of proteins in trehalose and other sugar formulations [5,10–14]. However, this simple view of the protein stabilization neglects the intrinsically heterogeneous nature of glass-forming liquids [15–21] on the nanoscopic dimensions of the protein molecules and the expected variations in this dynamic heterogeneity associated with the fragility of glass formation. Moreover, Crowe and coworkers [22,23] have emphasized the importance of strong hydrogen bond interactions between proteins and sugars, such as trehalose, to achieve effective coupling between the sugar solution and the protein. Caliskan *et al.* [24] have suggested that protein stability is enhanced by making the preservative formulation a stronger glass-forming liquid. Specifically, the amplitude of protein molecular motions, as measured by the Debye-Waller factor, within the glass can be reduced, and the protein preservation times can correspondingly be increased, by adding a small amount of glycerol to the trehalose solution [25,26]. This effect has been interpreted, by Caliskan *et al.* [24], as being due to the glycerol making the trehalose-glycerol mixture a stronger glass former, thus indicating a general principle for improving the cryopreservation times of proteins.

It has been demonstrated that glycerol alone suppresses protein (lysosyme) molecular motions at cryogenic temperatures better than glassy trehalose, but this trend inverts at high temperatures where the glycerol acts to enhance (i.e., "plasticize") protein conformational fluctuations [27–29]. Antiplasticization has been observed previously in a number of polysaccharides mixtures [30–33] and in synthetic polymers [34–38]. Einfeldt and coworkers [39–41] and Lourdin *et al.* [30–32] found antiplasticization in polysaccharides enriched by water and glycerol-water mixtures. Subsequent work by Lourdin *et al.* [31] indicated that glycerol slows down the secondary relaxation process of maltose up to concentrations of about 0.28 mass fraction. At higher concentration of glycerol, the secondary relaxation process of maltose merges with the primary structural relaxation process of glycerol, and only plasticization is apparent. Antiplasticiza-

*Electronic address: jack.douglas@nist.gov
†Electronic address: jan.obrzut@nist.gov

tion in synthetic polymers is normally accompanied by negative deviations from volume additivity upon mixing (i.e., the solutions densify upon mixing) that are symptomatic of antiplasticization. Lourdin and coworkers [32] considered the volumetric changes in glycerol maltose mixtures and found a density increase upon mixing that exhibited a maximum near a 0.2 solvent mass fraction. This finding is in good qualitative accord with previous observations on antiplasticization in synthetic polymers. Experience with synthetic polymers indicates that densification upon mixing does not universally indicate the existence of antiplasticization [35,36]. Synthetic polymer antiplasticizers impart rigidity into the matrix in which they are placed. In comparison to the statistical segment size of the polymer, antiplasticizers are relatively small molecules having rather a high glass transition temperature, which is typically greater than 220 K. Antiplasticizers interact strongly against phase separation making the mixture more thermodynamically stable [35–37]. The necessary conditions for antiplasticization seem to be satisfied for trehalose-glycerol mixtures and we thus use dielectric measurements to characterize these mixtures.

The present work is aimed at further elucidating the nature of glass formation in trehalose and glycerol formulations in the absence of proteins. This choice is predicated on previous findings that the dynamics of model proteins is largely "slaved" to the solvent in which it is placed [7–9] and observations of a correlation between the preservation time of model proteins in this type of formulation with the dynamical properties of the formulation alone [25,26].

II. MATERIALS AND MEASUREMENTS

Anhydrous α, α' trehalose and anhydrous glycerol were purchased from Sigma and Fluka, respectively, and used without further purification. The trehalose samples were prepared by melting them in an argon gas environment in a dry box at temperature of about 493 K. The mixtures of trehalose with glycerol were prepared by dispersing glycerol in the trehalose powder followed by a homogenization at 353 K overnight. After mixing, the samples were melted and then cooled rapidly on a cold plate to obtain glassy transparent films. Again, all samples were handled in an argon gas environment in the dry box.[1]

A. DSC measurements

Modulated differential calorimetry measurements (MDSC) were made with DSC 2910 from TA Instruments calibrated with water and indium. The heating rate was 2 K/min. These results were noted previously in a brief communication [42].

B. NMR measurements

Two nuclear magnetic resonance (NMR) spectrometers were employed, one noncommercial instrument was operated at 2.35 Tesla (100 MHz for protons) and the other was dedicated to ^{13}C observations with magic angle sample spinning (MAS). The other spectrometer is a Bruker Avance13 operating at 7.05 T (300 MHz for protons). For the T_{1H} measurements, the inversion recovery sequence was employed and detection was either indirect via cross-polarization to the ^{13}C nuclei or it was direct, using Fourier-transformed Bloch-decay proton spectra [43].

C. Dielectric measurements

Capacitance and loss tangent measurements in the frequency range of 100 Hz to 100 MHz were carried out using an Agilent 4294A Precision Impedance Analyzer. Calibration was performed with the extension adapter according to the manufacturer's specification for the 4294A. Before measurements, the test fixture was compensated to an electrical short, open and a 100 Ω load standard. The test fixture consisted of a parallel plate capacitor made of two glass slides with 11.9 mm diameter circular aluminum electrodes. The 100 nm thick electrodes were deposited on plasma-cleaned surfaces using vacuum evaporation. Approximately 200 μm thick spacers were attached to the glass slides and used to control the gap between the top and bottom electrodes. Solid film specimens were prepared in the dry box by melting samples between glass slides with electrodes, contacts, and spacers clamped together. After melting, the samples were cooled to obtain transparent glassy films. Liquid materials were injected to fill the gap between electrodes. The real part of the dielectric constant, ε', and the dielectric loss, ε'', were obtained from the measured complex capacitance and geometry of the test specimen. The relative standard uncertainty of the capacitance was assumed to be within the manufacturer's specification for the 4294A analyzer.

In the frequency range of 100 MHz to 18 GHz, the dielectric permittivity was obtained from one-port reflection coefficient measurements, which were carried out with a HP 8720D vector network analyzer [44,45]. Dielectric measurements were carried in a nitrogen gas environment in the temperature range of 220 K to 350 K using an environmental chamber, Model EC12 from Sun Electronic System. The specimen temperature was controlled to an uncertainty of ±0.5 K. The combined relative experimental uncertainty of the measured complex permittivity was within 8%, while the experimental resolution of the dielectric loss tangent measurements was about 0.005.

III. RESULTS

A. Dielectric measurements

Figure 1 illustrates the real (ε') and imaginary (ε'') part of permittivity as a function of frequency for a series of trehalose-glycerol mixtures as well as for pure trehalose and glycerol. The Havriliak-Negami (HN) relaxation function, defined by Eq. (1) below, has often been found to provide a good phenomenological description of dielectric relaxation data in glass-forming liquids [46,47] and this family of functions is a natural candidate for fitting our dielectric relaxation data. The real and imaginary parts of the dielectric relaxation data were fitted simultaneously to the HN expression,

[1]The materials and equipment identified in this paper are for descriptive purposes only and do not imply endorsement by the National Institute of Standards and Technology.

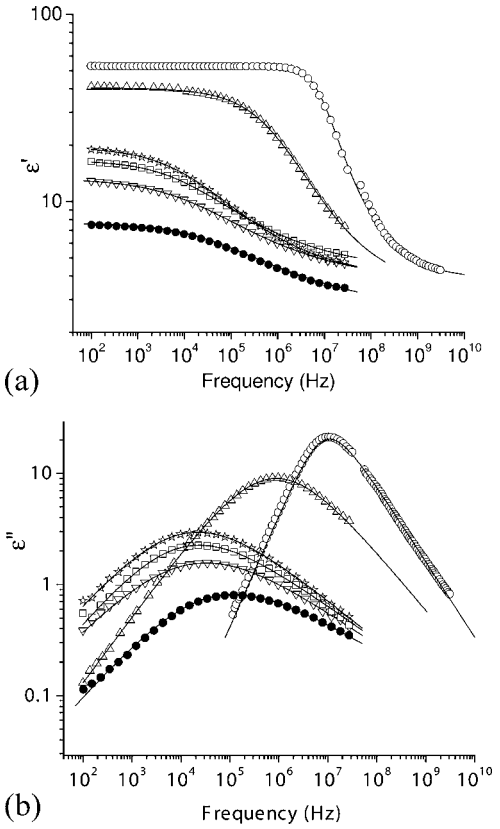

FIG. 1. (a) Real part ε', and (b) imaginary part ε'', of complex permittivity as a function of frequency for a series of trehalose-glycerol mixtures at 273 K. Symbols represent the experimental data while solid lines are fits to the Havriliak-Negami model; closed circles, trehalose; down triangles, x_w=0.15; squares x_w=0.24; stars x_w=0.36; up triangles x_w=0.47; and open circles, glycerol.

$$\frac{\varepsilon^*(\omega)-\varepsilon_\infty}{\Delta\varepsilon}=\frac{1}{[1+(i\omega\tau)^\alpha]^\gamma}, \tag{1}$$

using a nonlinear least-squares routine. The HN function parameters α and γ describe the extent of symmetric (α) and asymmetric (γ) broadening of the complex dielectric function, respectively, where α and γ are ($0<\alpha\leqslant 1$ and $0<\alpha\gamma\leqslant 1$). Equation (1) reduces to the well-known Debye expression where $\alpha=\gamma=1$. While the HN Eq. (1) is often referred to as an "empirical" relaxation function, recent modeling has linked parameters α and γ to the degree of intermittency in molecular movement and long-lived spatial fluctuations in local material properties (dynamic heterogeneity) [48–52], which gives some insight into the meaning of the fitted parameters. In this view, the exponent α is related to the temporal intermittency of molecular displacements while γ corresponds to long-lived spatial dynamic heterogeneities. Explicit computational models indicate that both α and γ of supercooled liquids decrease with decreasing temperature, as the fluid exhibits increased temporal and spatial heterogeneity [50–52].

The peak of ε'' at about 100 kHz [Fig. 1(b)] corresponds to a secondary relaxation in amorphous trehalose [53] and the solid lines represent the fitted permittivities from the HN equation. The fits are reasonably good and the corresponding HN parameters are summarized in the Table I for 250 K, 273 K, and 297 K. The qualitative effect of "antiplasticization" is seen as the movements of the ε'' peak to lower frequencies for a glycerol concentrations less than a 0.2 mass fraction, x_w.

Apart from the evident antiplasticization effect at lower glycerol concentrations, we see a general tendency of the relaxation parameters (α,γ in Table I) to approach larger values. It is seen that the dielectric relaxation process for pure trehalose is highly nonexponential and the dilution of trehalose with glycerol leads to an increasingly sharp distribution of relaxation times. The relaxation process becomes progressively more exponential in character with the addition of glycerol. We generally expect that the addition of a relatively strong glass-forming liquid (glycerol) to a fragile glass-forming liquid such as trehalose should lead to a mixture of intermediate fragility and tentatively associate this trend towards a more exponential relaxation in trehalose with an increasingly strong glass formation. Recent simulations have shown that antiplasticizers have the effect of reducing the fragility of glass-forming liquids, an effect consistent with our suggestion that the addition of glycerol makes trehalose a stronger glass former [52]. The dielectric strength, $\Delta\varepsilon$, relative to its high frequency value, ε_∞, is relatively small for trehalose. $\Delta\varepsilon$ lies in the range between 4 and 6 for temperatures between 250 K and 297 K and decreases further as the temperature is lowered, which is indicative of β-relaxation associated with local dipole fluctuation [54]. Glycerol, on the other hand, has a relatively high $\Delta\varepsilon$, in the range between 35 and 47, in the same temperature range and its value increases upon cooling, which indicates α relaxation, similar to that often found in network-forming hydrogen bonding liquids [55,56]. Our estimates of $\Delta\varepsilon$ for glycerol compare well with those of the classic study of Davidson and Cole [57].

Figure 2 shows the relaxation time τ of as a function of glycerol concentration for three different temperatures: 250 K, 273 K, and 297 K (Table I). The antiplasticizing effect becomes more pronounced at low temperatures, and the glycerol concentration at which the maximum in τ occurs itself depends on temperature. The relaxation time peaks at about 10^{-6} s for T=297 K, while for T=250 K the maximum is on the order of 10^{-3} s. At 250 K the peak is located near a 0.35 mass fraction of glycerol. Above this concentration range, τ decreases and the antiplasticizing effect apparently no longer exists. At these higher concentrations, however, the α-relaxation process of glycerol begins to overlap with relaxation process of trehalose.

The temperature dependence of the relaxation time τ is shown Fig. 3, where the relaxation time data is presented for pure trehalose, glycerol, and a series of trehalose-glycerol mixtures. The symbols correspond to τ data, while the lines represent linear regressions through the points. The relaxation time data for pure trehalose is well described by an Arrhenius temperature dependence $\tau=\tau_\infty\exp(E_a/RT)$, which is expected for the β-relaxation process, which is the focus of this study. The activation energy for the pure trehalose $E_{a\text{-treh}}$ approximately equals 59 kJ/mol, a value that is somewhat higher than a typical activation energy for the β-relaxation process in synthetic polymers (E_a in synthetic

TABLE I. Fitting parameters for a series of trehalose-glycerol mixtures at 250 K. Concentration of glycerol is given as a mass fraction x_w and mole fraction x_m.

x_w	x_m	τ (μs)	α	γ	$\Delta\varepsilon$	ε_∞
0	0	65.4	0.497	0.434	4.61	2.38
0.05	0.18	111	0.465	0.512	6.96	3.25
0.1	0.31	182	0.451	0.542	9.15	4.24
0.15	0.42	280	0.386	0.716	8.94	3.74
0.2	0.5	1260	0.402	0.669	9.60	3.51
0.24	0.56	816	0.471	0.578	12.1	4.19
0.36	0.70	1360	0.495	0.596	14.0	3.74
0.47	0.78	12	0.529	1.00	41.2	4.17
1.00	1.00	0.51	0.980	0.655	51.5	3.86

Fitting parameters for a series of trehalose-glycerol mixtures at 273 K

ξ_ω	ξ_μ	τ (μs)	α	γ	$\Delta\varepsilon$	ε_∞
0	0	4.68	0.500	0.519	5.02	2.57
0.05	0.18	6.72	0.514	0.530	7.26	3.36
0.1	0.31	13.9	0.510	0.495	9.72	4.08
0.15	0.42	11.6	0.467	0.654	9.51	3.78
0.2	0.5	16.9	0.437	0.793	10.2	3.69
0.24	0.56	16.7	0.535	0.592	12.4	4.29
0.36	0.70	13.6	0.511	0.708	15.8	3.86
0.47	0.78	0.213	0.596	0.894	37.0	3.50
1.00	1.00	0.0199	1.00	0.670	47.9	3.90

Fitting parameters for a series of trehalose-glycerol mixtures at 297 K

x_w	x_m	τ (μs)	α	γ	$\Delta\varepsilon$	ε_∞
0	0	0.750	0.543	0.417	5.74	1.92
0.05	0.18	0.946	0.602	0.393	8.16	2.79
0.1	0.31	1.35	0.603	0.350	11.5	2.76
0.15	0.42	0.789	0.539	0.576	10.5	3.53
0.2	0.5	1.04	0.540	0.616	11.1	3.45
0.24	0.56	1.20	0.611	0.478	13.8	3.60
0.36	0.70	0.363	0.539	0.704	18.3	3.35
0.47	0.78	0.00457	0.665	1.51	31.0	4.23
1.00	1.00	0.00135	1.00	0.674	38.9	3.79

polymers is usually in a range between 20 kJ/mol and 50 kJ/mol [54]). Our estimate of $E_{a\text{-treh}}$ agrees, however, with reports for other carbohydrates [33,39], so that larger values of E_a seem to be normal for carbohydrates. The relaxation time fits an Arrhenius law well up to a glycerol mass fraction of about $x_w \approx 0.5$. At higher glycerol concentrations, the β-relaxation process becomes increasingly masked by the α-relaxation of glycerol and these plots show considerable curvature. The curvature becomes large in the limit of pure glycerol, for which we can fit our data to the Vogel-Fulcher-Tammann (VFT) relation [58], $\tau = A \exp[B/(T-T_0)]$, where $A = 3.69 \times 10^{-15}$ s, $B = 17.2$ kJ/mol, and $T_0 = 139$ K, which is appropriate for an α-relaxation process. These parameter values agree well with previous reports for glycerol [59]. The concentration dependence of activation energy of the mixture $E_{a\text{-}mix}$ and the relaxation time pre-exponential factor of the mixture $\tau_{\infty\text{-}mix}$ are shown in the inset of Fig. 3.

It is apparent from Fig. 3 that for a fixed glycerol concentration there is a definite temperature at which antiplasticization first occurs upon cooling and we denote this temperature the "antiplasticization temperature," T_{ant}. This characteristic temperature is determined by the point at which the relaxation time for the mixture τ_{mix} crosses the relaxation time for pure trehalose τ_{treh} (see Fig. 3). For example, for a mixture having glycerol mass fraction x_w of 0.36, this slowing down effect of τ_{mix} only appears below 285 K (point of intersection of plot 3 with plot 1), while for $x_w = 0.1$, this crossover temperature T_{ant} increases to about 347 K. Determining T_{ant} in this way for a fixed x_w indicates that T_{ant} decreases monotonically with an increasing concentration as it is shown in

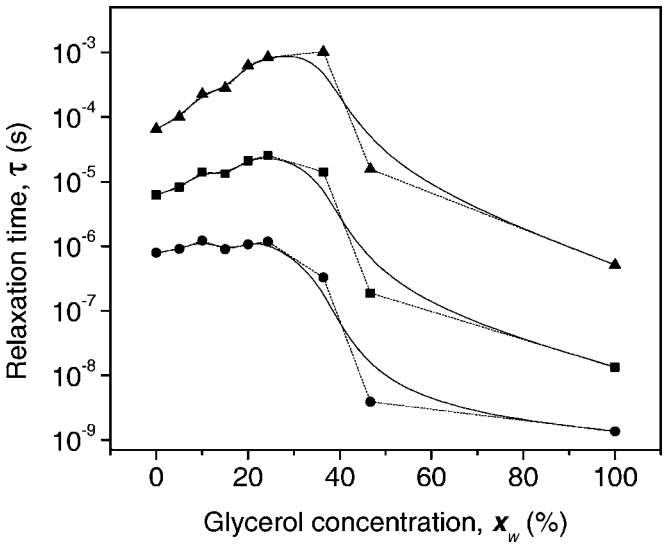

FIG. 2. Relaxation time vs concentration of glycerol at three different temperatures: triangles, 250 K; squares, 273 K; and circles, 297 K. Solid lines are guides for the eyes.

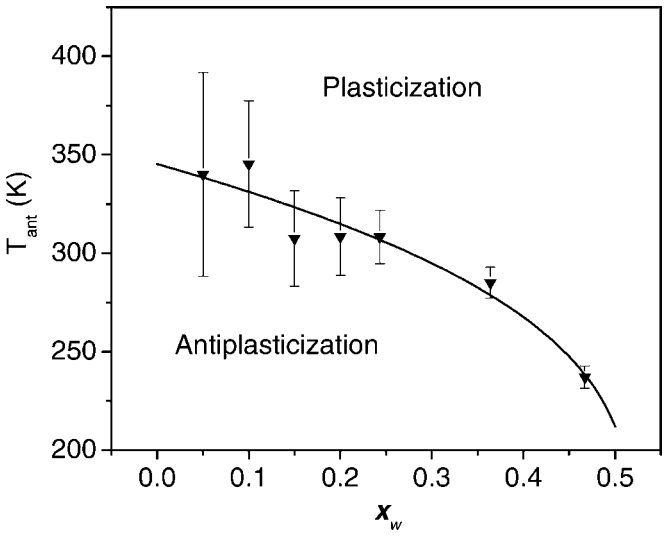

FIG. 4. A diagram of antiplasticization effect; the error bars are due to the procedure of determining the value of T_{ant}. Solid line represents the calculated results according to Eq. (2) with the following parameters: $T_0=397$ K, $\delta=-0.53$, and $x_w^*=0.52$.

Fig. 4. Thus, the antiplasticization effect only appears below the T_{ant} line. The effect bears a resemblance to the thermodynamic self-assembly transition which is governed by a compensation of entropic and enthalpic contributions to the free energy [60,61]. The T_{ant} results shown in Fig. 4 can be fitted reasonably well to an empirical expression,

$$T_{ant} \approx T_0/[1 + \delta \log(x_w^* - x_w)], \tag{2}$$

where x_w^* describes a characteristic concentration where T_{ant} begins to sharply decrease, x_w is mass fraction of glycerol, and δ is a parameter that describes the strength of this dropoff. A comparison of this functional description of T_{ant} with $T_0=397$ K, $\delta=-0.53$ and $x_w^*=0.52$ to the direct estimates of T_{ant} is plotted as a solid line in Fig. 4. Inverting Eq. (2) at a fixed temperature and taking $x_w<0.52$ as a variable, allows us to determine the plasticization concentration x_{wp} as a function of temperature.

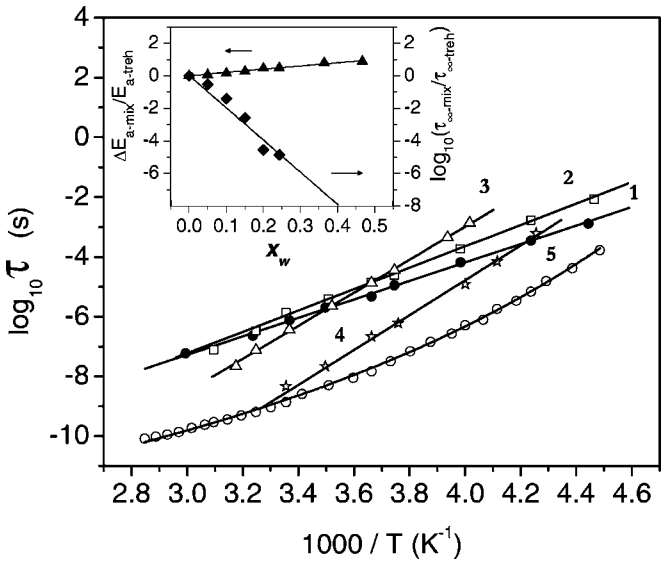

FIG. 3. Relaxation map for a series of trehalose-glycerol mixtures; (1), trehalose; (2), 0.1; (3), 0.36; (4), 0.47 mass fraction of glycerol in trehalose; (5), glycerol. Lines represent fitting to Arrhenius plot (trehalose) and VFT relation (glycerol). The inset presents concentration dependence of the activation energy of the secondary relaxation process in trehalose-glycerol mixtures normalized by the activation energy of pure trehalose and the extent of antiplasticization (see text).

Given these observations, it is natural to define the "dielectric antiplasticization factor" Θ as the relaxation times ratio, $\Theta=\tau_{mix}/\tau_{treh}$. The ratio Θ has the property of being greater than unity for antiplasticized mixtures and less than unity for plasticized mixtures. We can thus define "antiplasticization temperature" T_{ant} or the "plasticization concentration" x_{wp}, respectively, by the condition, Θ $(T=T_{ant})=1$, either at a fixed temperature and variable x_w or at fixed x_w and variable temperature. Otherwise, the magnitude Θ quantifies the "antiplasticization intensity." Figure 5 illustrates the variation of Θ as a function of temperature for several concentrations. For each concentration, these plots indicate well-defined regimes of antiplasticization ($\Theta>1$) and plasticization ($\Theta<1$), while T_{ant} defines a compensation temperature separating these regimes.

One of the properties of polymers exhibiting antiplasticization is that T_g normally decreases monotonically with the solvent concentration, despite the slowing down of the fast dynamics of the fluid by the antiplasticizer. Such a trend has previously been shown for maltose-glycerol mixtures [31]. Our DSC measurements on trehalose-glycerol mixtures, which were not subjected to freeze drying, also confirmed this expected trend. The T_g is approximately 392 K for pure trehalose, and then it decreases according to the formula $T_{g\text{-}mix}/T_{g\text{-}treh} \approx 1\text{-}1.12x_w$, approaching 304 K at $x_w=0.2$ [42].

While Θ provides an appropriate measure of the extent of antiplasticization, we seek other dielectric signatures that might be helpful in screening for antiplasticizing mixtures and in understanding the molecular origin of the effect. In

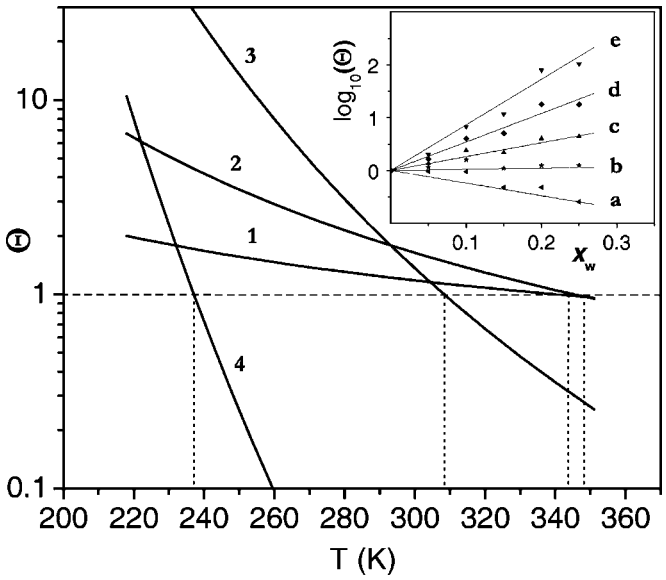

FIG. 5. Temperature dependence of dielectric antiplasticization factor, Θ, for several mixtures with glycerol concentrations; (1), 0.05; (2), 0.1; (3), 0.25; (4), 0.46 mass fraction. The insert presents Θ concentration dependence at the following temperatures: (a) 315 K; (b) 302 K; (c) 272 K; (d) 242 K; (e) 218 K.

the inset to Fig. 6, we show the concentration dependence of dielectric strength $\Delta\varepsilon$ for the three different temperatures considered previously (250 K, 273 K, and 297 K), relative to the value of $\Delta\varepsilon_{treh}$. It is seen that $\Delta\varepsilon_{mix}$ continuously increases with glycerol concentration. Normalizing $\Delta\varepsilon_{\mathrm{mix}}$ by $\Delta\varepsilon_{treh}$ indicates that at low concentrations the slope of $\Delta\varepsilon_{mix}/\Delta\varepsilon_{treh}$ versus x_w, the "intrinsic dielectric strength" $[\Delta\varepsilon]$ [62] is rather insensitive to temperature indicating a coherence between the molecular relaxation process in the mix and in trehalose. Although $[\Delta\varepsilon]$ quantifies the differential amount by which glycerol alters the dielectric properties

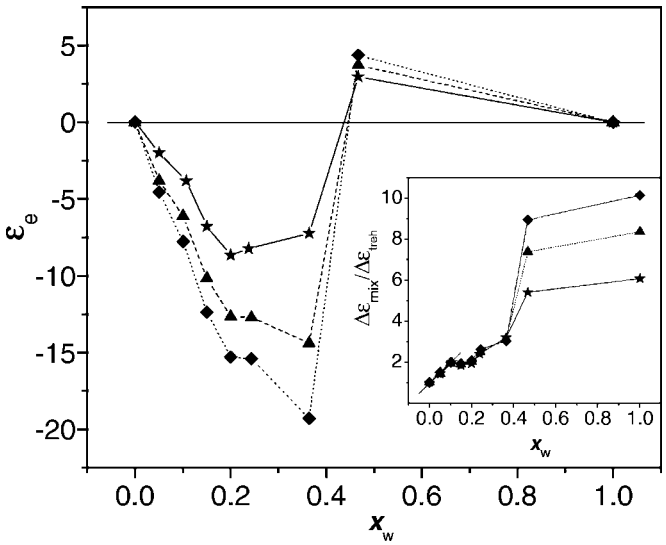

FIG. 6. Excess permittivity for the trehalose-glycerol mixtures vs glycerol concentration. Dielectric strength of the secondary relaxation process is shown in the insert; diamonds, 250 K; triangles, 273 K; and stars, 297 K.

of the trehalose-glycerol mixture, this quantity seems to provide little information directly relating to antiplasticization. In Fig. 6, we show the deviation of the observed $\Delta\varepsilon_{mix}$ from its value deduced from an ideal system exhibiting perfect random mixing and random particle orientation. Specifically, we focus on deviations from this average mean field $\Delta\varepsilon_{mix}$ by exploiting the excess permittivity ε_e of the mixture [63,64],

$$\varepsilon_e = \Delta\varepsilon_{mix} - x_m\Delta\varepsilon_{glc} + (1 - x_m)\Delta\varepsilon_{treh}, \tag{3}$$

where $\Delta\varepsilon_{mix}$ is the dielectric strength of the mixture (see Table I) and the mole fraction glycerol x_m is defined as $x_m = x_w/M_{glc}/[x_w/M_{glc} + (1-x_w)/M_{treh}]$. The relative molecular masses of glycerol and trehalose are M_{glc}=92.09 g/mol and M_{treh}=378.39 g/mol. If ε_e is zero, then the relaxation rate of the mixture is the arithmetic mean of the relaxation rates of pure components weighted by their molar fractions, and that intermolecular interaction are either effectively absent or do not affect the electric polarization in the mixture. Figure 6 shows that antiplasticization of trehalose by glycerol is accompanied by a drop in ε_e at low and moderate glycerol concentrations. This effect can be attributed to strong polar intermolecular interactions between trehalose and glycerol. At about 0.36 glycerol mass fraction, which corresponds to a stoichiometry composition that is two glycerol molecules to one trehalose molecule, ε_e sharply increases, apparently due to a change in dipole ordering.

B. NMR measurements

The 25 MHz ^{13}C cross-polarization magic angle spinning (CPMAS) spectrum of trehalose is illustrated in Fig. 7. Plots 7(a)–7(e) refer to glassy trehalose while plot 7(f) corresponds to crystalline trehalose. The development of crystallinity evidently has a clear signature in the NMR measurements. The NMR spectra corresponding to the case where the glassy and crystalline states coexist have similar characteristics to Fig. 7(f) so that NMR provides a powerful tool for monitoring for the occurrence of crystallization in our samples.

The dielectric loss spectra of the trehalose-glycerol mixtures, subjected to freeze-drying as in many of the protein preservation formulations, exhibit an additional peak at frequencies below 100 Hz that is absent in the mixtures without freeze-drying. In the NMR spectrum of glassy trehalose [65], there are three resonances apparent, with intensity ratios close to 1:4:1. By analogy to assignments in cellulose, the resonances near 62 ppm, 93 ppm, and 72 ppm are assigned, respectively, to the two pendent hydroxymethyl carbons (C6's), to the two anomeric carbons which are each bonded to two oxygen atoms (C1's), and to the remaining eight ring carbons (C2's-C5's). We found that the C6 resonance decays are significantly faster than the other resonances. However, the spectral density of motions with correlation times near 2×10^{-6} s, where the dielectric measurements place the center of the β relaxation, gives rise to only a weak feature in the NMR measurements. Secondary relaxation in glassy trehalose thus appears to be governed by small-amplitude motions that are not strongly localized at C6, and we suggest that they involve the entire glucopyranose ring. Further experimental and computational studies of the molecular origin of the fast relaxation process associated with the antiplasti-

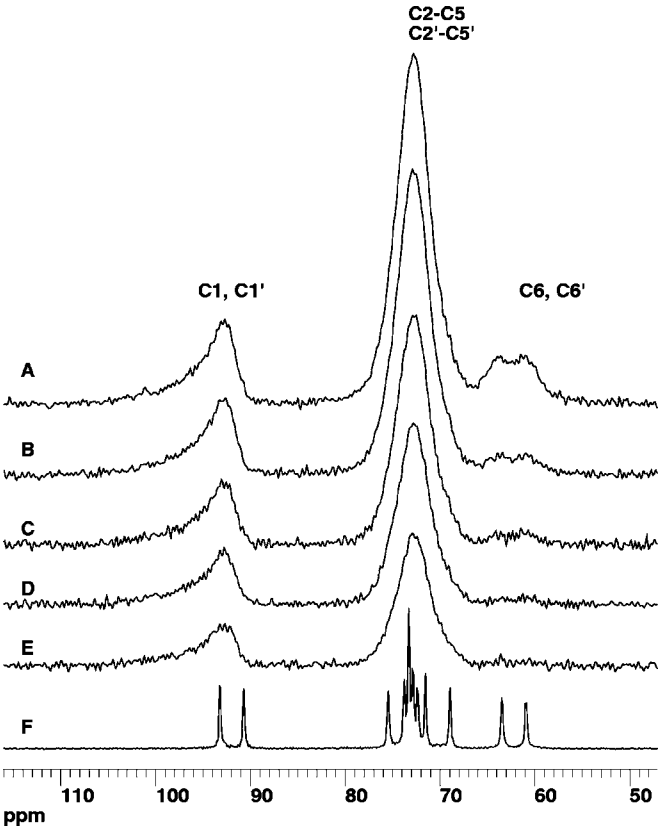

FIG. 7. Illustration of the 25 MHz ^{13}C CPMAS spectrum of trehalose. Glassy state trehalose [spectra (a)–(e)]; crystalline trehalose, (f). Decay times are 2 ms (a), 1 s (b), 3.5 s (c), 6 s (d), and 10 s (e).

cization effect would evidently provide insights into this phenomenon.

IV. DISCUSSION

A. Concentration and temperature dependence of the antiplasticization parameter, Θ

The physical interpretation of antiplasticization parameter Θ simplifies considerably when the relaxation time is described by an Arrhenius temperature dependence, which is normally the case for β-relaxation processes. In particular, we may express Θ as,

$$\Theta = \frac{\tau_{mix}}{\tau_{treh}} = \frac{\tau_{\infty\text{-}mix}\exp(E_{a\text{-}mix}/RT)}{\tau_{\infty\text{-}treh}\exp(E_{a\text{-}treh}/RT)}. \quad (4)$$

According to inset of Fig. 3, the activation energy ratio $E_{a\text{-}mix}/E_{a\text{-}treh}$ increases almost linearly with the glycerol concentration x_w. A comparison of the linear relation,

$$(E_{a\text{-}mix} - E_{a\text{-}treh})/E_{a,treh} \approx [E_a]x_w, \quad (5)$$

with our experimental data is shown in the inset of Fig. 3, where the slope $[E_a]$, "intrinsic activation energy," is positive. We might think that an increase in $E_{a\text{-}mix}$ with x_w could only lead to a strong increase in Θ, but this intuitive reasoning neglects the fact that the pre-exponential factor τ_∞ in the Arrhenius function for τ exhibits its own strong concentration dependence. The inset of Fig. 3 shows that $\tau_{\infty\text{-}mix}$ for the trehalose-glycerol mixture decreases exponentially with x_w,

$$\tau_{\infty\text{-}mix}/\tau_{\infty\text{-}treh} \approx \exp([\tau_\infty]x_w), \quad (6)$$

where $[\tau_\infty]$ is negative. Evidently, it is the competition between these two concentration trends in the activation energy $E_{a\text{-}mix}$ and the relaxation time pre-exponential factor $\tau_{\infty\text{-}mix}$ that leads to the peaking of antiplasticization as a function of x_w at a fixed temperature. The nearly exponential concentration dependence of τ_∞ (x_w) further implies that Θ at a fixed temperature reduces to a simple exponential function,

$$\Theta = \exp\left\{\left(\frac{E_{a\text{-}treh}[E_a]}{RT} + [\tau_\infty]\right)x_w\right\} = \exp(Ax_w), \quad (7)$$

where coefficient $A=(E_{a\text{-}treh}[E_a])/RT+[\tau_\infty]$ describes the rate of change of antiplasticization with concentration. The inset to Fig. 5 shows the relaxation data, shown in Fig. 3, in terms of a semilog plot to emphasize comparison with Eq. (7).

Using Eq. (7), one can find the conditions for plasticization or antiplasticization. $A>0$ corresponds to the antiplasticization conditions, which are desirable from the biopreservation point of view. In contrast, $A<0$ corresponds to plasticization. The condition $\Theta=1$, and correspondingly $A=0$, defines the antiplasticization temperature, T_{ant}. Clearly, $[E_a]$ and $[\tau_\infty]$ must have opposite signs for a finite antiplasticization temperature to exist. In the case of trehalose-glycerol, $[E_a]$ is positive while $[\tau_\infty]$ is negative. In the inverted case, where E_a is negative and $[\tau_\infty]$ is positive, the antiplasticization occurs at high temperatures, above the glass transition, while the fluid has an enhanced fluidity in the low temperature glass regime.

Within the formal theoretical framework of the transition state theory [60], $\tau_{\infty\text{-}mix}/\tau_{\infty\text{-}treh}$ equals $\exp(-\Delta S_a/R)$. Consequently, Θ can be expressed in terms of the change in the activation free energy $\Delta G_{a\text{-}mix}$,

$$\Theta = \exp(\Delta G_{a\text{-}mix}/RT), \quad \Delta G_{a\text{-}mix} = \Delta E_{a\text{-}mix} - T\Delta S_{a\text{-}mix}. \quad (8)$$

Thus, T_{ant} corresponds to a compensation point between the enthalpic and entropic contributions to the free energy of activation so that the antiplasticization temperature T_{ant} generally equals

$$T_{ant} = \Delta E_{a\text{-mix}}/\Delta S_{a\text{-mix}}. \quad (9)$$

For trehalose-glycerol systems, this point is illustrated in Fig. 5 where plots 1 and 2 show Θ as a function of T using the tabulated values of $E_{a\text{-}mix}$ and $\tau_{\infty\text{-}mix}/\tau_{\infty treh}$ shown in Table II. It is seen that Θ extrapolates to unity at the temperature $T_{ant}(x_w \to 0) \approx 347$ K in the limit of x_w approaching zero. The concentration dependence of T_{ant} can be traced to deviations of $\Delta E_{a\text{-}mix}$ and $\Delta S_{a\text{-}mix}$ from the proportionality to x_w, as indicated in the inset of Fig. 3 and mentioned above. If a strict linear dependence of $\Delta E_{a\text{-}mix}$ and $\Delta S_{a\text{-}mix}$ on concentration is held, then Eq. (9) would imply that T_{ant} should be independent of composition [see Eq. (7)].

The antiplasticization effect that we described in the present paper is certainly not restricted to applications relating to the preservation of proteins in sugar formulations.

TABLE II. Activation E_a energy and pre-exponential factor $\tau_{\infty\text{-}mix}$ for glycerol trehalose mixtures at glycerol concentrations x_w.

x_w	$\tau_{\infty\text{-}mix}$ (s)	E_a (kJ/mol)
0	2.83×10^{-17}	59.1
0.05	8.19×10^{-18}	62.6
0.1	1.08×10^{-18}	68.5
0.15	7.20×10^{-20}	74.4
0.2	7.79×10^{-20}	86.1
0.24	3.93×10^{-22}	87.8
0.36	7.61×10^{-26}	105.9
0.47	7.76×10^{-29}	111.6

There is evidence for a plasticization-antiplasticization transition in the dynamics of synthetic polymer solutions where the addition of a polymer to a fragile polymer liquid, such as Aroclor can either plasticize or antiplasticize the solvent to which they are added depending on concentration [66]. The interpretation of this concentration dependence of the fast viscolelastic relaxation time scale of polymer solutions has been a long-standing paradox in theoretical description of polymer solutions. The elucidation of the origin of this phenomenon in terms of the concentration dependence of the thermodynamic parameters, as presented in our work, was not possible in these earlier works because the measurements probed a much lower frequency range where the overlapping the α- and β-relaxation processes led to non-Arrhenius temperature dependence.

The antiplasticization temperature is notably below T_g of the bulk fluid, so that antiplasticization is normally a phenomenon relevant to the glassy state of the mixture. In some systems, however, such as unentangled polystyrene-mineral oil mixtures mechanical relaxation measurements indicate antiplasticization at high temperatures, above T_g, and plasticization seems to occur at low temperatures [67]. Such an inversion of the temperature range over which antiplasticization occurs is expected from Eq. (7) when the signs of $[E_a]$ and $[\tau_\infty]$ are inverted.

B. Antiplasticization and the permittivity increment, ε_e

We noticed that at low and moderate glycerol concentrations the antiplasticization of trehalose by glycerol is accompanied by a drop in the excess permittivity increment ε_e (Fig. 6). Aqueous solutions of simple alcohols often exhibit a minimum in ε_e [68,69]. On the other hand, polar molecule additives that largely disrupt the hydrogen bound network structure of water, as in the case of the antifreeze-type cryopreservative dimethylsulfoxide (DMSO), exhibit positive ε_e [70,71]. Similar behavior indicating that ε_e is positive has been observed in mixtures of organic solvents that don't assemble a hydrogen bound network structure [63,64,72]. For example, mixtures of CCl_4 with either o-xylene or ethylbenzene, show positive ε_e variations at any concentration ratio [64]. The variation of ε_e in trehalose-glycerol mixtures shown in Fig. 6 indicates both ε_e features, a minimum and a maximum. Such complex behavior has been seen before in mixtures of pyrrolidinone with hexamethyl-phosphortriamide [73]. The positive values of ε_e at high glycerol concentrations ($x_w > 0.36$) are consistent with trehalose, making glycerol a more fragile liquid ("fragilifier"), as previously reported for trehalose added to water at low concentrations [74–77] and for DMSO added to water [70,71]. The sharp change in ε_e in Fig. 6 reflects the transition between a regime where glycerol antiplasticizes trehalose to one in which trehalose enhances the fragility of glycerol.

The trends we observe for antiplasticization in trehalose-glycerol formulations are remarkably similar to those observed in synthetic polymer materials where small strongly interacting and high glass transition additives are added to highly fragile glass-forming fluids exhibiting poor packing due to the stiff nature and irregular shapes of the molecules involved [35–37]. Glycerol has a relatively high glass transition temperature ($T_g = 186$ K) [78] compared to water $T_g = 136$ K [79] and many other small molecule liquids, and is capable of strong hydrogen bonding with the glassy trehalose so there is a physical analogy to synthetic polymeric systems exhibiting antiplasticization.

While the existence of an antiplasticization temperature has been recognized in previous measurements on carbohydrate formulations and synthetic polymers, this temperature was apparently not specifically defined or explicitly evaluated. The concentration where the antiplasticization changes to antiplasticization (0.2 to 0.3 glycerol mass fraction) seems to be typical in comparison to synthetic polymers that exhibit antiplasticization. This concentration range is also typical for previous observations of density maxima in mixtures of maltose and glycerol [32] and it is natural to expect similar behavior in the trehalose-glycerol system.

C. Complexities of the freeze-drying process

Freeze-drying, also known as lyophilization, is a dehydration process typically used to make preserving formulation from water solutions. Freeze-drying works by freezing the material and then reducing the surrounding pressure to allow the frozen water in the material to sublimate directly from the solid phase to gas [80,81]. We made a preliminary attempt to characterize the dielectric properties of our trehalose-glycerol mixtures subjected to freeze-drying, but found that these samples contained a number of additional relaxation processes in a frequency range intermediate between our β-relaxation process and the frequency range characteristic of large scale structural α relaxation. Moreover, the intensity and characteristic frequencies of these relaxation processes drifted slowly over the time scales of days. Evidently, freeze-drying imparts significant complexity to the molecular structure of these carbohydrate formulations and further studies will be necessary to understand what structural changes are occurring in these fluids. The amount of residual water left in the freeze-dried samples would seem to be a basic question that should be resolved in understanding these mixtures, especially given the hygroscopic nature of glycerol. In view of the significant structural and composition changes in the nature of the freeze-dried glycerol-trehalose formulations, we are satisfied with the agreement in

the qualitative common trends observed in these different investigations [25,26]. Future work should consider how the detailed history of the freeze-drying process influences the antiplasticization of the formulation and the resulting preservative properties. As we have shown, NMR is a valuable tool in monitoring crystallization and other ordering processes that occur in connection with the freeze-drying process.

V. CONCLUSION

The addition of glycerol to glassy trehalose increases the secondary dielectric relaxation time. According to our NMR results, the secondary relaxation in glassy trehalose is governed by small-amplitude motions involving the entire glucopyranose ring. Glycerol slows down these motions and antiplasticizes trehalose. We quantify this antiplasticization effect by determining the temperature dependence of the relaxation time governing the secondary relaxation time τ as function of temperature and glycerol concentration x_w.

The antiplasticization occurs only below a certain antiplasticization temperature (T_{ant}). This characteristic temperature decreases with an increase of glycerol concentration x_w. To measure the extent of antiplasticization, we introduced the dielectric antiplasticization factor Θ defined as the ratio of the relaxation times of the mixture to the relaxation time of pure glassy trehalose. The antiplasticization factor is greater than unity for antiplasticized mixtures and less than unity for plasticized mixtures. We find that the antiplasticization of trehalose is accompanied by a significant decrease in excess permittivity ε_e. Moreover, the sharp change in ε_e from negative to positive at x_w of about 0.36 reflects the transition from a regime where glycerol antiplasticizes trehalose to one in which the strong glass formation of glycerol is modulated by the fragile fluid trehalose. Our data is consistent with expectation that the addition of glycerol makes trehalose a stronger glass former and that the addition of trehalose to glycerol makes the mixture a strong glass former in the limits where the additive concentrations are low. Nevertheless, measurements at lower frequencies by dynamical mechanical or other methods are required to really prove that this expected behavior is true.

In biopreservation applications, it is important to realize that this type of antiplasticization of glassy liquids only exists at low temperatures and that the same additive can serve to plasticize rather than antiplasticize at higher temperatures. The temperature at which this change occurs evidently gives basic information for the effective preservation of biological materials as well as for the adjustment of the properties of synthetic glassy polymers under processing conditions and in their applications in the field. As T_{ant} was found to be well below the glass transition temperature of the trehalose glycerol mixture and to decrease with increasing glycerol concentration, we see that increasing the concentration of antiplasticizer requires a lower temperature for the antiplasticization to be effective in the sugar-glycerol formulations. Future work should consider the significance of T_{ant} in relation to the characteristic temperatures of glass formation in order to better understand this important phenomenon from a more fundamental perspective.

ACKNOWLEDGMENT

The authors would like to thank Dr. Bert W. Rust from Mathematical and Computational Sciences Division, NIST, for his expert help in solving the regression problems by means of regularization techniques.

[1] D. P. Miller, J. J. dePablo, and H. Corti, Pharm. Res. **14**, 578 (1997), and Refs. [5–7] therein.
[2] Y. C. Song, B. S. Khirabadi, F. Lightfoot, K. G. M. Brockbank, and M. J. Taylor, Nat. Biotechnol. **18**, 296 (2000).
[3] R. El Moznine, G. Smith, E. Polygalov, P. M. Suherman, and J. Brodhead, J. Phys. D **36**, 330 (2003).
[4] B. S. Chang, R. M. Beauvais, A. Dong, and J. F. Carpenter, Arch. Biochem. Biophys. **331**, 249 (1996); J. Buitink, I. J. van den Dries, F. Hoekstra, M. Alberda, and M. A. Hermiminga, Biophys. J. **79**, 1119 (2000).
[5] J. L. Green and C. A. Angell, J. Phys. Chem. **93**, 2880 (1989); see Ref. [10].
[6] G. M. Wang and A. D. J. Haymet, J. Phys. Chem. B **102**, 5341 (1998).
[7] A. Ansari, C. M. Jones, E. R. Henry, J. Hofrichter, and W. A. Eaton, Science **256**, 1796 (1992); see also Refs. [56–58] for further examples of the slaving of the protein dynamics to that of the solvent.
[8] A. P. Sokolov, H. Grimm, and R. Kahn, J. Chem. Phys. **110**, 7053 (1999).
[9] A. L. Tournier, J. Xu, and J. C. Smith, Biophys. J. **85**, 1871 (2003).
[10] J. L. Green, J. Fan, and C. A. Angel, J. Phys. Chem. **98**, 13780 (1994).
[11] L. N. Bell, M. J. Hageman, and L. M. Muraoka, J. Pharm. Sci. **84**, 707 (1995).
[12] R. M. H. Hatley, Pharm. Dev. Technol. **2**, 257 (1997).
[13] S. L. Shamblin, X. Tang, L. Chang, C. Hancock, and M. J. Pikal, J. Phys. Chem. B **103**, 4113 (1999).
[14] W. Wang, Int. J. Pharm. **203**, 1 (2000).
[15] M. D. Ediger, Annu. Rev. Phys. Chem. **51**, 99 (2000).
[16] I. Chang and H. Sillescu, J. Phys. Chem. B **101**, 8794 (1997).
[17] E. R. Weeks, J. C. Crocker, A. C. Levitt, A. Schofield, and D. A. Weitz, Science **287**, 627 (2000).
[18] W. K. Kegel and A. van Blaanderen, Science **287**, 290 (2000).
[19] C. Bennemann, C. Donati, J. Baschnagel, and S. C. Glotzer, Nature **399**, 246 (1999).
[20] A. I. Melcuk, R. A. Ramos, H. Gould, W. Klein, and R. D. Mountain, Phys. Rev. Lett. **75**, 2522 (1995).
[21] C. Donati, J. F. Douglas, W. Kob, S. J. Plimpton, P. H. Poole, and S. C. Glotzer, Phys. Rev. Lett. **80**, 2338 (1998).
[22] L. M. Crowe, D. S. Reid, and J. H. Crowe, Biophys. J. **71**, 2087 (1996).
[23] J. H. Crowe, J. F. Carpenter, and L. M. Crowe, Annu. Rev. Physiol. **60**, 73 (1998).
[24] G. Caliskan, A. Kisliuk, A. M. Tsai, C. L. Soles, and A. P.

Sokolov, J. Non-Cryst. Solids **307–310**, 887 (2002).
[25] M. T. Cicerone and C. S. Soles, Biophys. J. **86**, 3836 (2004).
[26] M. T. Cicerone, A. Tellington, I. Troust, and A. Sokolov, Bioprocess. Int. **1**, 36 (2003).
[27] C. A. Angel, K. F. Freed, and J. F. Douglas, Science **267**, 1924 (1995).
[28] A. M. Tsai, D. A. Neumann, and L. N. Bell, Biophys. J. **79**, 2728 (2000).
[29] A. Paciaroni, S. Cinelli, and G. Onori, Biophys. J. **83**, 1157 (2002).
[30] D. Lourdin, H. Bizot, and P. Colonna, J. Appl. Polym. Sci. **63**, 1047 (1997).
[31] D. Lourdin, S. G. Ring, and P. Colonna, Carbohydr. Res. **306**, 551 (1998).
[32] D. Lourdin, P. Colonna, and S. G. Ring, Carbohydr. Res. **338**, 2883 (2003).
[33] T. R. Noel, S. G. Ring, and M. A. Whittam, J. Phys. Chem. **96**, 5662 (1992).
[34] W. J. Jackson, Jr. and J. R. Caldwell, Adv. Chem. Ser. **48**, 185 (1965); J. Appl. Polym. Sci. **11**, 211 (1967); **11**, 227 (1967).
[35] L. M. Robeson, Polym. Eng. Sci. **9**, 277 (1969).
[36] Y. Maeda and D. R. Paul, J. Polym. Sci., Part B: Polym. Phys. **25**, 957 (1987); **25**, 981 (1987); **25**, 1005 (1987).
[37] P. Bergquist, Y. Zhou, A. A. Jones, and P. T. Inglefield, Macromolecules **32**, 7925 (1999).
[38] K. L. Ngai, R. W. Rendell, A. F. Yee, and D. J. Plazek, Macromolecules **24**, 61 (1991).
[39] J. Einfeldt, D. Meißner, and A. Kwasniewski, Prog. Polym. Sci. **26**, 1419 (2001).
[40] J. Einfeldt, A. Kwasniewski, D. Klemm, R. Dicke, and L. Einfeldt, Polymer **41**, 9273 (2000).
[41] J. Einfeldt, D. Meißner, A. Kwasniewski, and L. Einfeldt, Polymer **42**, 7049 (2001).
[42] M. T. Cicerone, J. Obrzut, A. Anopchenko, and C. L. Soles, Bull. Am. Phys. Soc. **42**, W1704 (2003).
[43] D. L. VanderHart and G. C. Campbell, J. Magn. Reson. **134**, 88 (1998).
[44] J. Obrzut and A. Anopchenko, IEEE Trans. Instrum. Meas. **53**, 1197–1201 (2004).
[45] J. Obrzut, A. Anopchenko, and R. Nozaki, Proceedings of the IEEE Conference on Instrum. and Meas., 16–19 May 2005, Ottawa, Canada 2, 1530 (2005).
[46] K. S. Cole and R. H. Cole, J. Chem. Phys. **9**, 341 (1941); **10**, 98 (1942).
[47] S. Havriliak and S. Negami, Polymer **8**, 161 (1967).
[48] V. V. Novikov and V. P. Privalko, Phys. Rev. E **64**, 031504 (2001).
[49] Y. E. Ryabov, Y. Feldman, N. Shinyashiki, and S. Yagihara, J. Chem. Phys. **116**, 8610 (2002).
[50] J. F. Douglas and J. B. Hubbard, Macromolecules **24**, 3163 (1991).
[51] J. F. Douglas, J. Phys.: Condens. Matter **11**, A329 (1999).
[52] R. A. Riggleman, K. Yoshimoo, J. F. Douglas, and J. J. de-Pablo, Phys. Rev. Lett. **97**, 045502 (2006).
[53] A. De Gusseme, L. Carpentier, J. F. Willart, and M. Descamps, J. Phys. Chem. B **107**, 10879 (2003).
[54] A. Schonhals, in *Dielectric Spectroscopy of Polymeric Materials, Fundamentals and Applications*, edited by J. P. Runt, J. J. Fitzgerald (American Chemical Society, Washington, DC, 1997), Chap. 3.
[55] A. Catenaccio, Y. Daruich, and C. Magallanes, Chem. Phys. Lett. **367**, 669 (2003).
[56] S. J. Bass, W. I. Nathan, R. M. Meighan, and R. H. Cole, J. Phys. Chem. **68**, 509 (1964).
[57] D. W. Davidson and R. H. Cole, J. Chem. Phys. **19**, 1484 (1951).
[58] H. Vogel, Z. Phys. **22**, 645 (1921); G. S. Fulcher, J. Am. Ceram. Soc. **8**, 339 (1923).
[59] P. Lunkenheimer, U. Schneider, R. Brand, and A. Loidl, Contemp. Phys. **41**, 15 (2000).
[60] N. E. Hill, W. E. Vaughhan, A. H. Price, and M. Davis, *Dielectric Properties and Molecular Behavior* (Reinhold, London, 1969), pp. 69–71; S. Gladstone, K. J. Laidler, and H. Eyring, *The Theory of Rate Processes* (New York, McGraw-Hill, 1941).
[61] K. Van Workum and J. F. Douglas, Phys. Rev. E **71**, 031502 (2005).
[62] J. F. Douglas and E. J. Garboczi, Adv. Chem. Phys. **91**, 85 (1995).
[63] D. Bertolini, M. Cassettari, C. Ferrari, and E. Tombari, J. Chem. Phys. **108**, 6416 (1998).
[64] A. H. Buep, M. B. R. Paz, and J. L. Touron, J. Mol. Liq. **45**, 237 (1990).
[65] P. Zhang, A. N. Klymachyov, S. Brown, J. G. Ellington, and P. J. Grandinetti, Solid State Nucl. Magn. Reson. **12**, 221 (1998).
[66] T. P. Lodge, J. Phys. Chem. **97**, 1480 (1993).
[67] S. L. Anderson, E. A. Grulke, P. T. DeLassus, P. B. Smith, C. W. Kocher, and B. G. Landes, Macromolecules **28**, 2944 (1995).
[68] F. Corradini, A. Marchetti, M. Tagliazucchi, L. Tassi, and G. Tosi, J. Chem. Soc., Faraday Trans. **90**, 1089 (1994).
[69] T. P. Iglesias, J. Peon Fernandez, J. Martin-Herrero, and A. Seoane, J. Mol. Liq. **95**, 147 (2002).
[70] C. M. Kinart, W. J. Kinart, A. Cwiklinska, and D. Checinska, J. Mol. Liq. **100**, 65 (2002).
[71] A. Luzar, J. Mol. Liq. **46**, 221 (1990).
[72] V. P. Pawar and S. C. Mehrotra, J. Mol. Liq. **108**, 95 (2003).
[73] P. Pirila-Honkanen and P. Ruosteuso, Thermochim. Acta **184**, 65 (1991).
[74] C. Branca, S. Magazù, F. Migliardo, and P. Migliardo, Physica A **304**, 314 (2002).
[75] C. Branca, S. Magazu, G. Maisano, P. Migliardo, V. Villari, and A. K. Sokolov, J. Phys.: Condens. Matter **11**, 3823 (1999).
[76] S. Magazu, V. Villari, P. Migliardo, G. Maisano, and M. T. F. Telling, J. Phys. Chem. B **105**, 1851 (2001).
[77] S. Magazu, P. Migliardo, and C. Mondelli, Biophys. J. **86**, 3241 (2004).
[78] M. K. Carpenter, D. B. Davies, and A. J. Matheson, J. Chem. Phys. **46**, 2451 (1967).
[79] D. Kivelson and G. Tarjus, J. Phys. Chem. B **105**, 6620 (2001).
[80] J. D. Mellor, *Fundamentals of Freeze-Drying* (Academic Press, New York, 1978).
[81] T. A. Jennings, *Lyophilization-Introduction and Basic Principles* (Interpharm Press, Buffalo Grove, IL, 1999).